FATIGUE CRACK PROPAGATION IN TYPES 304 AND 308 STAINLESS STEEL AT ELEVATED TEMPERATURES

MATERIALS

KEYWORDS: *Type 304 stainless steel, fatigue, cracks, filler metals, Type 308 stainless steel, stresses, aging, high temperature, welded joints*

D. T. RASKE and C. F. CHENG *Argonne National Laboratory*
Materials Science Division, 9700 South Cass Avenue, Argonne, Illinois 60439

Received August 23, 1976
Accepted for Publication January 5, 1977

The fatigue crack-growth behavior of Type 304 stainless-steel base metal and Type 308 stainless-steel weld metal at elevated temperature was investigated using axially loaded single-edge-notch specimens. The crack-growth rates were determined and are presented as a function of the stress-intensity factor range. Both the base- and weld-metal specimens were tested in the as-received (or as-welded) and thermally aged condition. The results indicate that the crack-growth rates in the weld metal are significantly lower than in the base metal. In addition, aging at 593°C for 1000 h improved the resistance to fatigue crack growth in both the base and weld metals.

INTRODUCTION

Austenitic stainless steels fabricated by welding for use in liquid-metal fast breeder reactors (LMFBRs) pose numerous questions related to the mechanical integrity of the structural components. One question relevant to the design of these components is how will the weld metal behave in relation to the base metal when cracks are present? Before investigating this problem, consideration of the LMFBR operating conditions and structural uses indicated that test of weld- and base-metal samples at 593°C (1100°F) in air would provide an adequate data base to compare the two metals. Furthermore, since prolonged exposure of these steels in this environment results in the precipitation of carbides,[1] thermal aging prior to testing was considered as one of the variables to be investigated.

The purpose of the present study was to determine the fatigue crack-growth resistance in the base- and weld-metal portions when Type 304 stainless-steel plates are joined by shielded-metal arc welding with Type 308 stainless-steel filler metal. The filler metal was designated as Type 308 CRE because of the controlled residual elements that improve its strength and ductility.[2,3] The present paper summarizes the results of crack-growth-rate tests on these metals in the aged and unaged conditions at 593°C (1100°F).

EXPERIMENTAL PROCEDURE

The chemical compositions of the Type 304 stainless-steel plates and Type 308 CRE weld metal used in the present study are listed in Table I. Microstructures for both metals in the aged and unaged condition are shown in Fig. 1. The average grain size in the base metal was ~120 μm. The microstructure of the weld metal consisted of 3.8 to 4.2% ferrite distributed in an austenite matrix. Plates 60 mm ($2\frac{3}{8}$ in.) thick were manually welded by Combustion Engineering, Inc., using the shielded-metal arc process. The weld joint was a double "U" groove type. The welds were prepared and tested in accordance with the requirements of the American Society of Mechanical Engineers (ASME) Code.

Axially loaded single-edge-notch (SEN) specimens were made from the base and weld metal as shown in Fig. 2. Because these plates were cross-rolled, identification of the original rolling direction was not possible. Both the base- and weld-metal specimens were tested in the as-received (as-welded) and thermally aged conditions. The aging was performed in an inert atmosphere at 593°C (1100°F) for 1000 h.

With the exception of three tests, all of the specimens used were rigidly gripped at their ends. A three-post die set (Fig. 3) was used to

prevent rotation and translation of the specimen during testing. Specimens CE23B3, CE40W2, and CE41W4 were pin loaded with grips similar to those recommended in American Society for Testing and Materials (ASTM) Standard E399 (Ref. 5). Most of the specimens had crack-starter notches, as shown in Fig. 2. The fatigue cracks that initiated from these notches were grown to ~1.3 mm (0.05 in.) before crack-growth-rate measurements were begun. This resulted in a total crack plus notch length of ~3.8 mm (0.150 in.) when data acquisition began. The depth of the crack-starter notches for the pin-loaded specimens was increased to 3.05 mm (0.120 in.), with a maximum radius of 76.0 μm (0.003 in.). In these specimens, the initial notch plus fatigue crack length prior to crack-growth-rate measurements was 5.08 mm (0.200 in.).

All specimens were tested in uniaxial tension at a load ratio, P_{min}/P_{max}, of 0.05 and a temperature of 593°C (1100°F). Specimen heating was accomplished by an induction coil that operated at 455 kHz. The coil, shown in Fig. 4, was constructed to provide a flat temperature profile over a distance of 13 mm (0.5 in.) on either side of the crack plane. Power to the coil was provided by a Lepel high-frequency induction heater and controlled by a thermocouple welded to the specimen. The thermocouple was located just below the line of crack growth at the opposite end of the crack-starter notch.

The tests were performed in an MB Electronics servo-controlled hydraulic testing machine. Water-cooled grips provided thermal protection to the load cell. A triangular waveform and cyclic frequency of 0.5 Hz were used in all tests.

The load history used for precracking and during the tests is shown in Table II. Crack lengths were measured on the side of the specimen using a traveling microscope with a magnification of 40×. The crack-length measurements were aided by a series of perpendicular scribe marks at 1.3-mm (0.050-in.) intervals on each side of the specimens. These marks also constituted the extension interval for crack-length measurement. Except for the pin-loaded specimens, the crack lengths were measured on one side only. The average difference in crack length measured on each side of the pin-loaded specimens was <6%. No gross deviations of the crack plane from the plane of symmetry were observed. It is estimated that the accuracy of crack-length measurements was within ~9% of the true value. This was determined by post-test observations of the fracture surface on those specimens subjected to changes in the continuity of loading at each scribe mark.

TABLE I

Chemical Composition of Type 304 Stainless-Steel Plate and Type 308 CRE Weld Metal

Metal	Content (wt%)														
	C	Mn	P	S	Si	Cr	Ni	Mo	Cb	Ti	Co	Cu	B	V	N_2
Type 304 plate, HT.300380-1A	0.058	1.60	0.016	0.011	0.55	18.68	8.44	---	---	---	---	---	---	---	---
Type 304 plate, HT. 600414-1A	0.061	1.48	0.016	0.014	0.64	18.88	9.56	---	---	---	---	---	---	---	---
Type 308 CRE, Batch 2	0.051	1.87	0.042	0.009	0.60	20.10	10.14	0.24	Cb + Ta <0.01	0.06	0.07	0.17	0.007	0.10	0.042

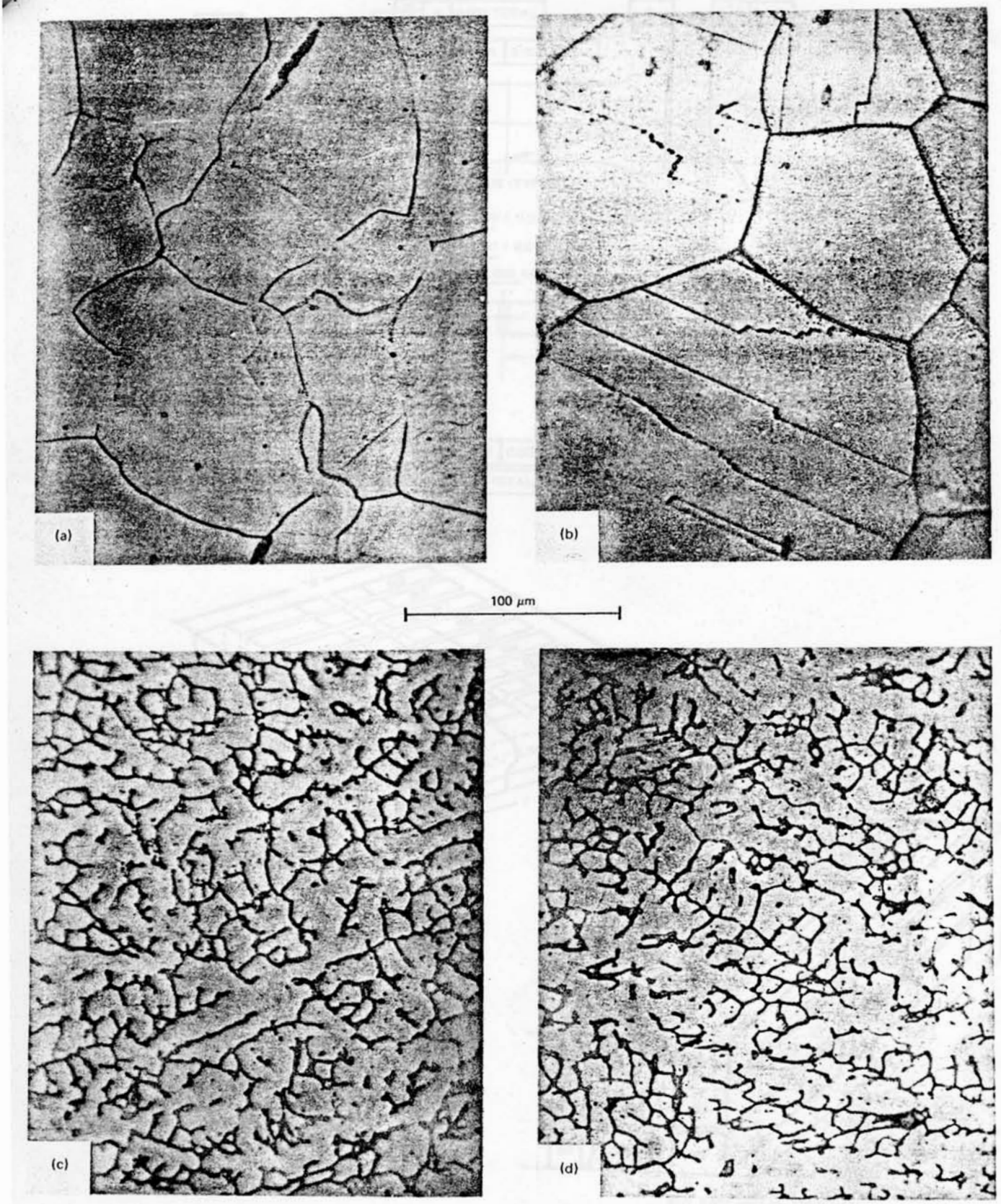

Fig. 1. Microstructure of Type 304 stainless-steel base-metal and Type 308 stainless-steel weld-metal specimens: (a) base-metal as-received, (b) base-metal aged, (c) weld-metal as-welded, and (d) weld-metal aged.

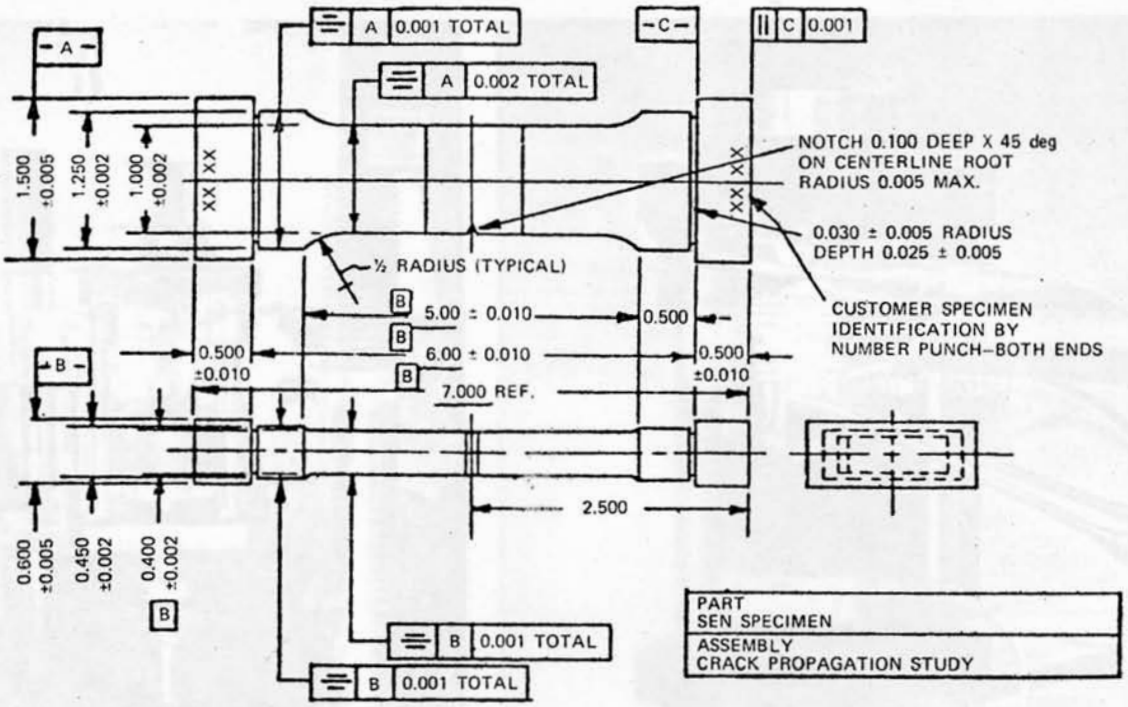

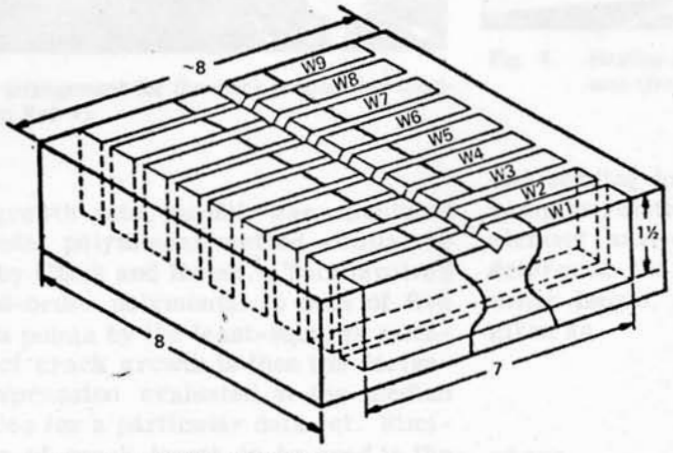

SEN WELD-METAL SPECIMEN

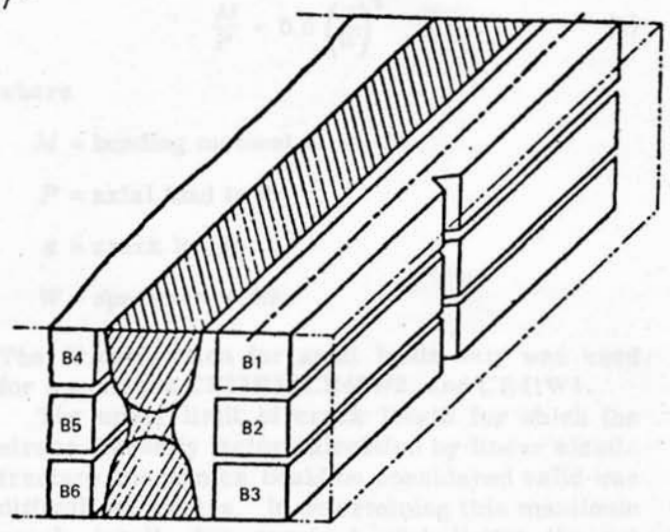

SEN BASE-METAL SPECIMEN

Fig. 2. Single-edge-notch (SEN) weld- and base-metal specimens.

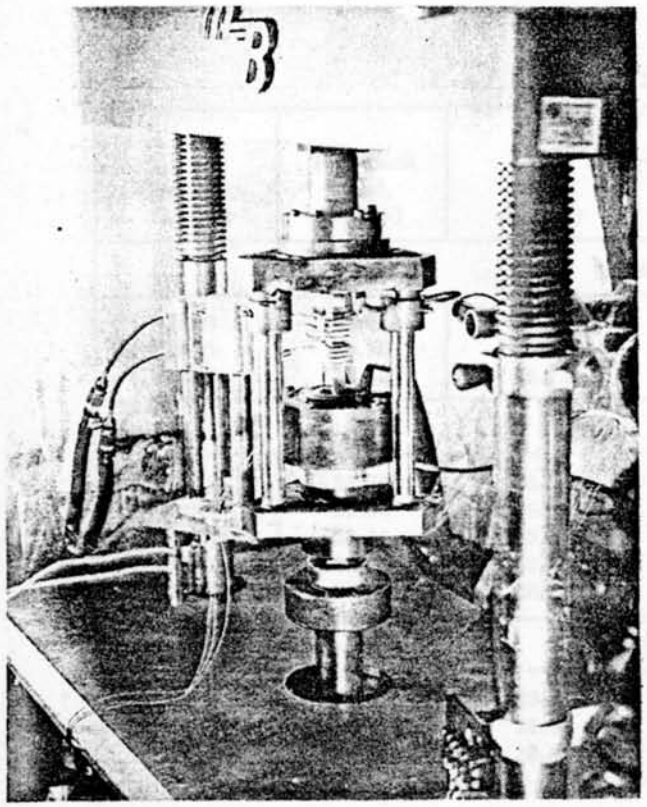

Fig. 3. Gripping arrangement for the crack-propagation specimen (from Ref. 4).

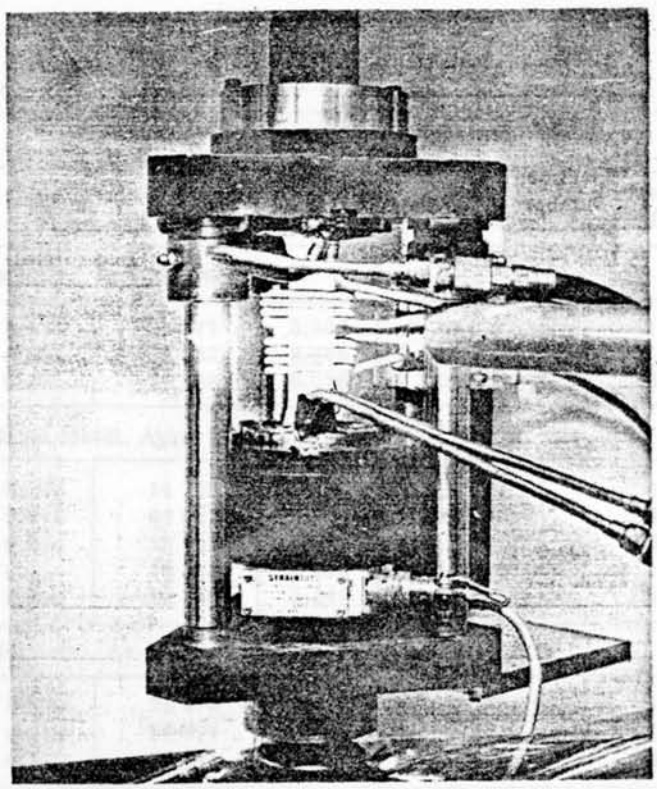

Fig. 4. Heating arrangement for the crack-propagation specimen (from Ref. 4).

The crack-growth rate, da/dN, was calculated by an incremental polymonial method similar to that described by Clark and Hudak.[6] This involves fitting a second-order polymonial to sets of five successive data points by the least-squares method. The rate of crack growth is then the derivative of this expression evaluated at the median number of cycles for a particular data set. Similarly, the value of crack length to be used in the calculation of the stress-intensity factor range, ΔK, is the estimated value, $\hat{a}$, at this number of cycles. After the first set of five data points is evaluated, this method is applied to the next set, and a new polymonial is determined. This is continued until each set of successive data points has been analyzed. The result is a smooth fit through all of the data and values of da/dN and $\hat{a}$ for each data point except the first two and last two. Hence, a test that consists of, for example, 11 observations would result in 7 calculated values each for da/dN and $\hat{a}$.

The stress-intensity factor for the fixed-end specimens was determined from the relation

$$K_{\text{total}} = K_{\text{axial}} - K_{\text{bending}} \quad , \tag{1}$$

where K_{axial} and K_{bending} are the usual stress-intensity values for SEN specimens under axial and bending loads, respectively.[7] Because of the complex relationship between these loads, a finite-element analysis of the specimen was used to determine the relationship between the axial load, crack length, and bending moment. The result is given as

$$\frac{M}{P} = 0.6\left(\frac{a}{W}\right)^2 \quad , \tag{2}$$

where

M = bending moment in in.-lb

P = axial load in lb

a = crack length

W = specimen width.

The K calibration for axial loads only was used for specimens CE23B3, CE40W2, and CE41W4.

The upper limit of crack length for which the stress-intensity factor calculated by linear elastic fracture mechanics could be considered valid was difficult to assess. In determining this maximum crack length, the approach that limits the net section stresses (axial or axial plus bending) to some arbitrary percentage of the yield strength appears to be overconservative. Therefore, an

TABLE II

Fatigue Crack-Growth-Rate Test Data

Specimen Number	Precrack Load, ΔP (kN)	Test Load, ΔP (kN)	Initial Value		Final Value		Load Change to Record Crack Length[a]
			a/W	Number of Cycles	a/W	Number of Cycles	
Base Metal, As-Received							
CE32B3	21.35	21.35	0.228	20 777	0.508	32 577	1
CE32B1	34.30	34.30	0.202	9 532	0.475	15 605	1
CE32B5	33.72	33.72	0.211	11 738	0.515	16 857	2
Base Metal, Aged							
CE33B1	33.76	33.76	0.216	14 139	0.510	19 272	4
CE33B6	25.58	25.58	0.213	36 072	0.522	47 599	3
CE33B4	33.81	33.81	0.244	12 948	0.439	17 198	2
CE34B2	33.98	33.98	0.194	10 460	0.420	16 150	1
CE23B3	25.35	25.35	0.198	21 813	0.449	33 138	5
Weld Metal, As-Welded							
CE39W9	33.81	33.81	0.202	28 979	0.512	34 766	1
CE39W8	25.31	25.31	0.214	57 977	0.508	81 221	1
CE41W6	33.81	33.81	0.192	28 241	0.538	37 503	2
Weld Metal, Aged							
CE29W2	25.31	25.31	0.311	116 237	0.527	121 894	3
CE39W5	34.03	34.03	0.235	26 150	0.520	32 245	5
CE42WA-1	33.90	33.90	0.170	20 735	0.482	33 997	5
CE42WB-1	33.81	33.81	0.178	24 902	0.472	39 837	5
CE42WB-2	25.35	33.81, 25.35	0.217	50 592	0.508	78 293	5
CE42WC-1	33.85	33.85	0.187	30 732	0.514	44 968	5
CE42WC-2	25.40	33.81	0.171	32 610	0.484	60 476	5
CE42WD-1	33.98	33.98	0.171	32 912	0.510	48 176	5
CE42WD-2	25.35	34.03	0.187	40 968	0.482	68 243	5
CE42WE-1	33.81	33.90	0.189	25 140	0.493	39 497	5
CE40W2	25.35	25.35	0.198	40 320	0.502	56 627	1
CE41W4	25.35	25.35	0.212	93 211	0.506	111 823	1

[a] The numeral 1 indicates no load change and continuous cycling; 2 indicates that the test was stopped and restarted at each scribe mark; 3 indicates a 1-min tension hold (P_{max}) at each scribe mark; 4 indicates frequency reduction to 0.005 Hz (5 mHz) for one cycle at each scribe mark; and 5 indicates hold at zero load for ~1 min at each scribe mark.

approach similar to that used by Corwin[8] was adopted. This method limits the amount of crack-tip necking by terminating the test when specimen thinning or "dimpling" is apparent.

RESULTS AND DISCUSSION

The results of our investigation are presented in terms of the empirical relationship of Paris and Erdogan[9]:

$$\frac{da}{dN} = C\,(\Delta K)^m \quad , \tag{3}$$

where C and m are parameters that depend on the material and environment. Figures 5 and 6 are logarithmic plots of da/dN versus ΔK for the base metal in the as-received and aged condition and weld metal in the as-welded and aged condition, respectively. The solid line in these figures is the regression-analysis line of log (da/dN) on log (ΔK). The dashed lines represent the 95% confidence intervals of a new observation or result, da/dN, for a given value of ΔK. Note that because these intervals account for the variability of the new observation as well as that of the original sample, they will be wider than would be

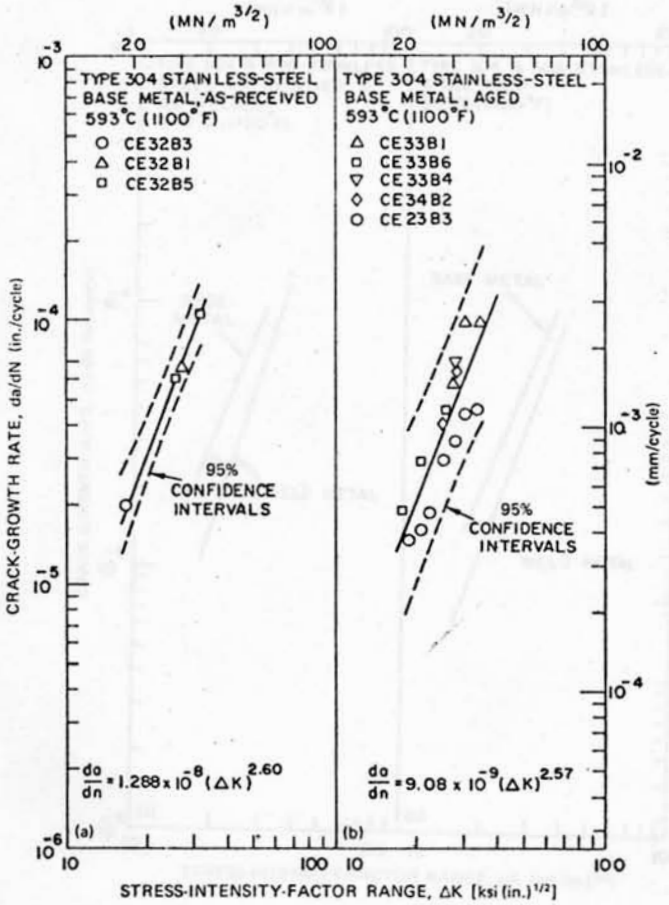

Fig. 5. Fatigue crack-growth rate as a function of the stress-intensity range for (a) as-received and (b) aged Type 304 stainless steel.

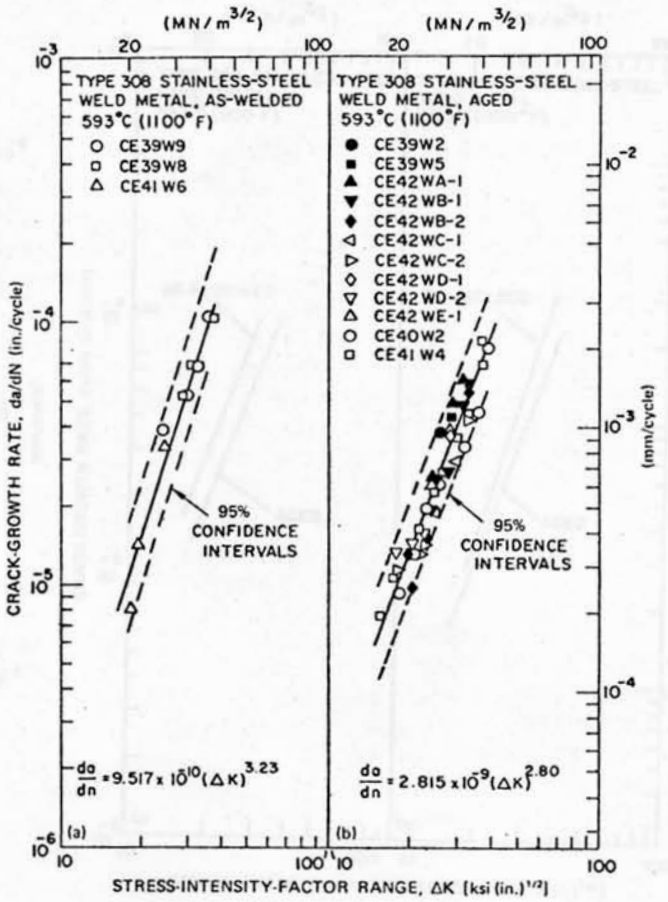

Fig. 6. Fatigue crack-growth rate as a function of the stress-intensity range for (a) as-welded and (b) aged Type 308 stainless steel.

predicted on the basis of the original sample data alone.[10] The equations of the regression lines are given as follows for ΔK in ksi (in.)$^{1/2}$ and da/dN in in./cycle:

Base metal, as-received:

$$\log\left(\frac{da}{dN}\right) = -7.890\ (\pm 0.169) + 2.602\ (\pm 0.121)\log(\Delta K)$$

or

$$\frac{da}{dN} = 1.29 \times 10^{-8}\,(\Delta K)^{2.60} \quad , \tag{4}$$

Base metal, aged:

$$\log\left(\frac{da}{dN}\right) = -8.042\ (\pm 0.594) + 2.571\ (\pm 0.420)\log(\Delta K)$$

or

$$\frac{da}{dN} = 9.08 \times 10^{-9}\,(\Delta K)^{2.57} \quad , \tag{5}$$

Weld metal, as-welded:

$$\log\left(\frac{da}{dN}\right) = -9.021\ (\pm 0.342) + 3.230\ (\pm 0.236)\log(\Delta K)$$

or

$$\frac{da}{dN} = 9.52 \times 10^{-10}\,(\Delta K)^{3.23} \quad , \tag{6}$$

Weld metal, aged:

$$\log\left(\frac{da}{dN}\right) = -8.550\ (\pm 0.197) + 2.801\ (\pm 0.139)\log(\Delta K)$$

or

$$\frac{da}{dN} = 2.82 \times 10^{-9}\,(\Delta K)^{2.80} \quad , \tag{7}$$

Figure 7 shows a comparison, based on the regression lines, of the crack-growth rates in the base and weld metal for the as-received (or as-welded) and aged conditions. The effect of aging, for both the base and weld metal, is shown in Fig. 8. A comparison of the results of the

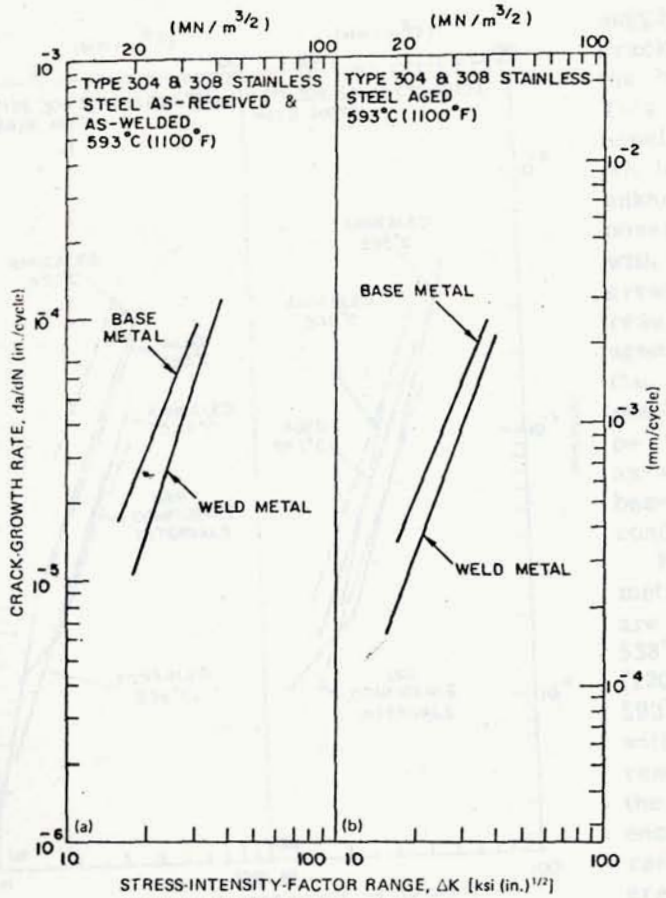

Fig. 7. Comparison of fatigue crack-growth rates in (a) as-received and as-welded and (b) aged Types 304 and 308 stainless steel.

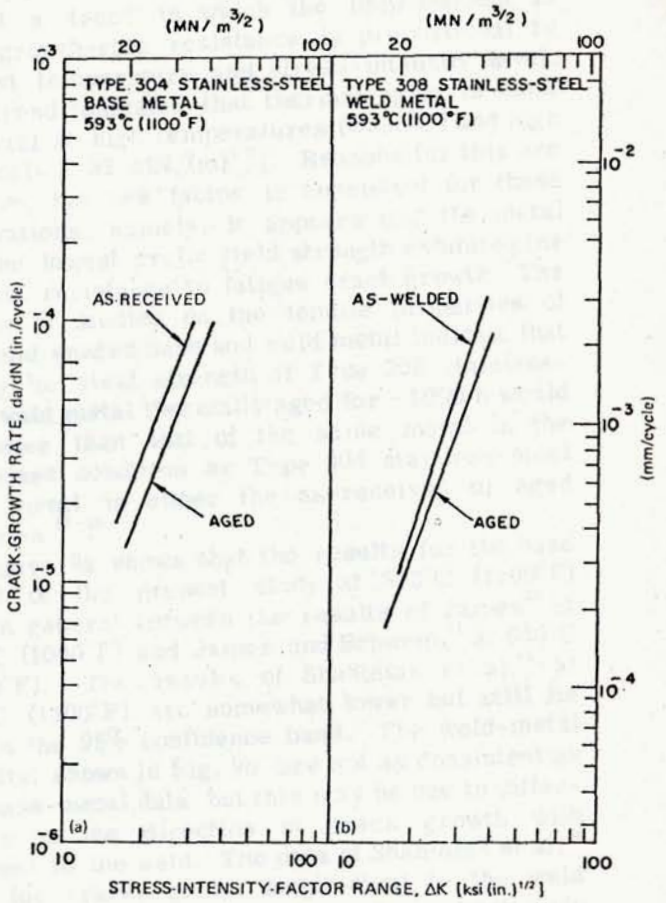

Fig. 8. Effect of thermal aging on fatigue crack-growth rates in (a) Type 304 stainless-steel base metal and (b) Type 308 stainless-steel weld metal.

present study and data from the literature[11-14] on annealed Types 304 and 308 stainless steel is shown in Fig. 9. The weld-metal cracks in the present study and those reported by James[13] are parallel to the longitudinal weld axis and extend from the surface toward the root of the weld. The data of Shahinian et al.[14] show that cracks in their specimens grow parallel to the longitudinal weld axis.

As can be observed from Figs. 5 and 6, the scatter in the aged base-metal test data is considerably greater than in any of the other cases and is approximately twice that of the aged weld-metal test data. This is attributed to the various means used to enhance the crack front at each crack-extension interval to more accurately measure crack length (Table II). In the other tests, more consistent means were used to determine the crack length at each interval, and, consequently, the specimen-to-specimen scatter is much lower. Although the aged base-metal scatter appears to be considerable, comparison with other investigations indicates that it is not excessive. In the report by Clark and Hudak[6] on the variability in fatigue crack-growth-rate tests, the average variance of residuals from the regression line of da/dN on ΔK for 14 different laboratories that tested the same specimens was 0.027. The variance of the residuals for the aged base-metal data of the present study is somewhat less, 0.020.

Different specimen loadings (fixed versus pin ends) could also affect the scatter of the data if the bending moment, crack length, axial load relation [Eq. (2)] were in error. This systematic error is not observed, and in fact the scatter for both types of specimens made from the weld metal is random. Hence, it appears that the major sources of scatter in the data, particularly for the aged base metal, are different load changes and hold times at the end of each increment of crack extension (Table II).

As shown in Fig. 7, the weld metal has a lower crack-growth rate than the base metal in both the as-welded (as-received) and aged conditions. This

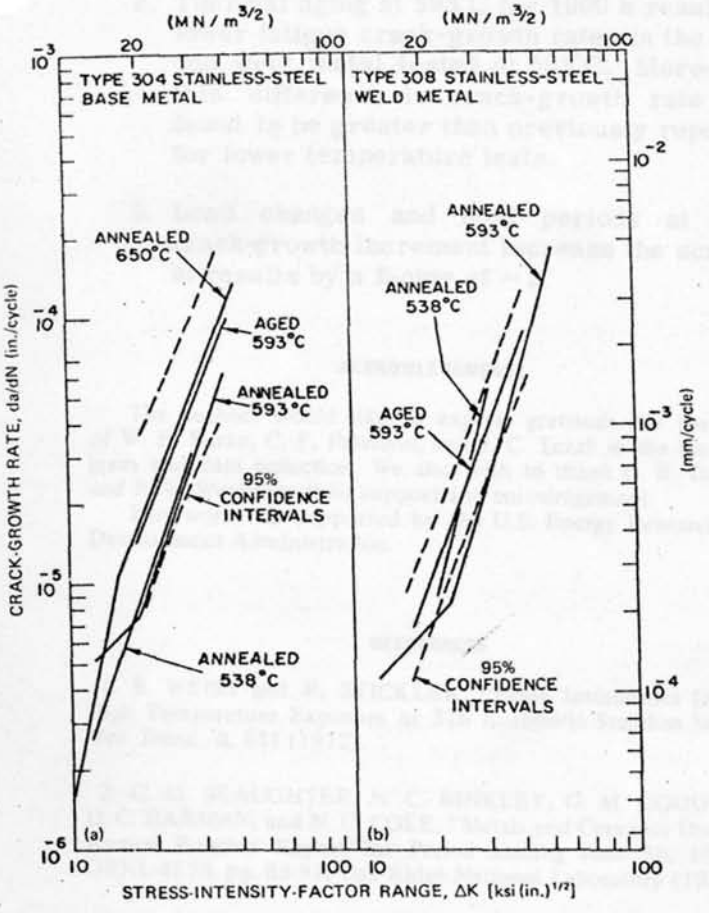

Fig. 9. Comparison of crack-growth rates in (a) Type 304 stainless steel tested at 650°C (annealed) (Ref. 11), 593°C (annealed) (Ref. 14), 538°C (annealed) (Ref. 12), and 593°C (aged) and (b) Type 308 stainless steel tested at 593°C (annealed) (Ref. 14), 538°C (annealed) (Ref. 13), and 593°C (aged).

result is consistent with the results of other investigations[13,14] on the same base-weld metal combination and supports the contention that existent design rules may be safely applied to components that contain welds. We join James[13] and Shahinian et al.[14] in suggesting that this higher crack-growth resistance is due to the fine duplex microstructure of the weld.

In both the base and weld metal shown in Fig. 8, aging resulted in lower crack-growth rates than observed for specimens in the as-received or as-welded condition. In addition, these rates are statistically different, over the range of growth rates tested, above the 99% level.[15] The effect of aging on crack-growth rates in these metals at room temperature and 538°C (1000°F) was also investigated by James.[16] His findings indicate that thermal aging was beneficial only at the higher temperature, and even then the effect was slight. These results[16] and those of the present study suggest a trend in which the improvement in crack-growth-rate resistance is proportional to the test temperature and stress-intensity level. This trend indicated that thermal aging is most beneficial at high temperatures (≥538°C) and high ΔK levels [>22 MN/(m)$^{3/2}$]. Reasons for this are unknown, but one factor is consistent for these observations, namely, it appears that the metal with the lowest cyclic yield strength exhibited the greatest resistance to fatigue crack growth. The results of studies on the tensile properties of aged and unaged base and weld metal indicate that the cyclic yield strength of Type 308 stainless-steel weld metal thermally aged for ~1000 h would be lower than that of the same metal in the as-welded condition or Type 304 stainless-steel base metal in either the as-received or aged condition.[17-19]

Figure 9a shows that the results for the base metal of the present study at 593°C (1100°F) are in general between the results of James[12] at 538°C (1000°F) and James and Schwenk[11] at 650°C (1200°F). The results of Shahinian et al.[14] at 593°C (1100°F) are somewhat lower but still lie within the 95% confidence band. The weld-metal results, shown in Fig. 9b, are not as consistent as the base-metal data, but this may be due to differences in the direction of crack growth with respect to the weld. The data of Shahinian et al.[14] are for cracks grown longitudinal to the weld direction, whereas the data from the present study and the work of James[12] are for cracks grown through the thickness of the weld.

SUMMARY AND CONCLUSIONS

The fatigue crack-growth resistance of Type 304 stainless-steel base metal and Type 308 stainless-steel weld metal at 593°C (1100°F) has been investigated. Specimens of both materials in the as-received (or as-welded) and thermally aged conditions were tested. The crack-growth rates were found to be exponentially related to the stress-intensity factor range, ΔK. This relation, determined by regression analysis, was statistically appropriate and generally provided a good fit to the data. Confidence levels for new crack-growth rate observations were estimated, and comparisons of mean crack-growth rates were made.

The results of the present investigation suggest the following conclusions:

1. The fatigue crack-growth rates at 593°C (1100°F) in the Type 308 stainless-steel weld metal are statistically lower than in the Type 304 stainless-steel base metal in both the aged and as-welded (or as-received) conditions.

2. Thermal aging at 593°C for 1000 h results in lower fatigue crack-growth rates in the base and weld metal tested at 593°C. Moreover, this difference in crack-growth rate was found to be greater than previously reported for lower temperature tests.

3. Load changes and hold periods at each crack-growth increment increase the scatter in results by a factor of ~3.

ACKNOWLEDGMENTS

The authors would like to express gratitude for the help of W. F. Burke, C. F. Peterson, and J. C. Tezak in the test program and data reduction. We also wish to thank D. R. Diercks and R. W. Weeks for their support and encouragement.

This work was supported by the U.S. Energy Research and Development Administration.

REFERENCES

1. B. WEISS and R. STICKLER, "Phase Instabilities During High Temperature Exposure of 316 Austenitic Stainless Steel," *Met. Trans.*, **3**, 851 (1972).

2. G. M. SLAUGHTER, N. C. BINKLEY, G. M. GOODWIN, D. C. HARMAN, and N. C. COLE, "Metals and Ceramics Division Annual Progress Report for Period Ending June 30, 1970," ORNL-4570, pp. 88-91, Oak Ridge National Laboratory (1970).

3. G. M. GOODWIN, N. C. COLE, and R. G. BERGGREN, "Metals and Ceramics Division Annual Progress Report for Period Ending June 30, 1972," ORNL-4820, pp. 73-75, Oak Ridge National Laboratory (1972).

4. R. W. WEEKS, D. R. DIERCKS, and C. F. CHENG, "ANL Low-Cycle Fatigue Studies–Program, Results, and Analysis," ANL-8009, Argonne National Laboratory (Nov. 1973).

5. "Standard Method of Test for Plane-Strain Fracture Toughness of Metallic Materials (E399-72)," *Annual Book of ASTM Standards*, Part 31, pp. 955-974, American Society for Testing and Materials, Philadelphia (1972).

6. W. G. CLARK, Jr. and S. J. HUDAK, Jr., "Variability in Fatigue Crack Growth Rate Testing," *J. Test. Eval.*, **3**, 454 (1975).

7. W. F. BROWN and J. E. SRAWLEY, "Plane Strain Crack Toughness Testing of High Strength Metallic Materials," *ASTM STP 410*, American Society for Testing and Materials, Philadelphia (1967).

8. W. R. CORWIN, "Subcritical Crack Growth of $2\frac{1}{4}$Cr–1 Mo Steel," ORNL-5106, pp. 147-155, Oak Ridge National Laboratory (July 1975).

9. P. PARIS and F. ERDOGAN, "A Critical Analysis of Crack Propagation Laws," *J. Basic Eng.*, **85**, 528 (1963).

10. J. NETER and W. WASSERMAN, *Applied Linear Statistical Models*, Richard D. Irwin, Inc., Homewood, Illinois (1974).

11. L. A. JAMES and E. B. SCHWENK, Jr., "Fatigue Crack Propagation Behavior of Type 304 Stainless Steel at Elevated Temperatures," *Met. Trans.*, **2**, 491 (1971).

12. L. A. JAMES, "A Survey of the Effect of Heat-to-Heat Variations upon the Fatigue-Crack Propagation Behavior of Types 304 and 316 Stainless Steels," HEDL-TME 75-37, Hanford Engineering Development Laboratory (May 1975).

13. L. A. JAMES, "Crack Propagation Behavior in Type 304 Stainless Steel Weldments at Elevated Temperature," *Weld. Res.*, **52**, 173s (1973).

14. P. SHAHINIAN, H. H. SMITH, and J. R. HAWTHORNE, "Fatigue Crack Propagation in Stainless Steel Weldments at High Temperature," *Weld. Res.*, **51**, 527s (1972).

15. "A Guide for Fatigue Testing and the Statistical Analysis of Fatigue Data," *ASTM STP 91-A*, American Society for Testing and Materials, Philadelphia (1963).

16. L. A. JAMES, "Effect of Thermal Aging upon the Fatigue-Crack Propagation of Austenitic Stainless Steels," *Met. Trans.*, **5**, 831 (1974).

17. R. T. KING, E. BOLLING, and B. McNABB, Jr., "Tensile Properties of Aged SMA Type 308 CRE Stainless Steel FFTF Vessel Test Welds," ORNL-4936, pp. 145-152, Oak Ridge National Laboratory (Oct. 1973).

18. C. R. BRINKMAN and G. E. KORTH, "Heat-to-Heat Variations in the Fatigue and Creep-Fatigue Behavior of AISI Type 304 Stainless Steel, and the Fatigue Behavior of Type 308 Stainless Steel Weld Metal," ANCR-1097, Aerojet Nuclear Company (May 1973).

19. J. M. STEICHEN and A. L. WARD, "High Strain Rate Tensile Properties of Type 308 SMA Weld Metal," *Weld. Res.*, **54**, 130s (1975).